International Journal of Simulation, Optimization & Modelling
ISSN: 3083-967X

One-Year Performance Analysis of a 3000 Wp Grid-Connected PV System in Tropical Climate

Syafrizal[1], Asri Gani[2], Muhtadin[3], Yuni Lisafitri[4]

[1]Department of Environment Engineering, Universitas Serambi Mekkah, Banda Aceh, 23245, Indonesia
[2]Department of Chemical Engineering, Universitas Syiah Kuala, Banda Aceh 23111, Indonesia
[3]Department of Mechanical Engineering, Universitas Abulyatama Aceh, Aceh Besar, 23372, Indonesia
[4]Environmental Engineering Department, Institut Teknologi Sumatera, Bandar Lampung, Indonesia

Corresponding Author: asri_gani@usk.ac.id

Abstract
This study presents a comprehensive performance evaluation of a 3000 Wp grid-connected photovoltaic (PV) system over a one-year operational period. The objective is to analyze system behavior under real environmental conditions using detailed statistical and graphical methods. The methodology includes daily and monthly assessments of irradiance, power output, temperature, voltage, and system losses. A total of 15 figures were used to visualize the system's behavior, including input/output relationships, performance ratio trends, and power and temperature distributions. Results show an average annual reference incident energy of 4.846 kWh/m²/day, with peak values in February (6.0 kWh/m²/day) and minimum values in June (4.0 kWh/m²/day). The produced useful energy averaged 4.06 kWh/kWp/day, with total system losses of 0.79 kWh/kWp/day comprised of 12.9% collection loss and 3.3% inverter/system loss. The Performance Ratio (PR) was consistently high at 0.838, reflecting efficient energy conversion across all seasons. Power output was most frequently distributed between 1500 W and 2500 W, peaking around 2000 W. Thermal and electrical stability were confirmed with module temperatures mostly ranging from 30°C to 50°C and voltage concentrated around 150 V. The novelty of this study lies in its integration of cumulative tail distributions, voltage/temperature histograms, and irradiance correlation analysis methods not commonly used together in existing literature. These findings confirm the system's reliability and offer valuable insight into operational optimization and design strategies. The study contributes a practical, data-driven reference for PV performance benchmarking under tropical climate conditions.

Article Info
Received: 25 March 2025
Revised: 15 April 2025
Accepted: 20 April 2025
Available online: 21 May 2025

Keywords
Photovoltaic System Performance
Solar Energy Yield
Performance Ratio
Energy Loss Analysis
Tropical Climate PV Monitoring

1. Introduction

The rapid global transition toward renewable energy has placed photovoltaic (PV) systems at the forefront of sustainable electricity generation. As concerns over climate change and fossil fuel depletion intensify, solar power continues to emerge as a clean, abundant, and increasingly cost-effective alternative. Particularly in tropical regions, where solar irradiance is consistently high, PV systems have demonstrated great promise in meeting energy demand while reducing environmental impact.

Numerous studies have investigated PV system performance under varying climatic conditions. Researchers have focused on system efficiency, temperature effects, seasonal irradiance variations, and inverter losses (Bhavani, Vijaybhaskar Reddy, Mahesh, & Saravanan, 2023; Iqbal, Rosdi, Muhtadin, Erdiwansyah, & Faisal, 2025; Jalaludin, Kamarulzaman, Sudrajad, Rosdi, & Erdiwansyah, 2025; Muhtadin, Rosdi, Faisal, Erdiwansyah, & Mahyudin, 2025). For instance, temperature-induced losses can significantly affect system yield in hot climates, while the role of inverter efficiency in determining total energy output is also crucial (Aghaei et al., 2022; Bahagia, Nizar, Yasin, Rosdi, & Faisal, 2025; Pranoto, Rusiyanto, & Fitriyana, 2025; Yana, Mufti, Hasiany, Viena, & Mahyudin, 2025). Others have explored optimization strategies through maximum power point tracking (MPPT) and system orientation adjustments (Gani, Saisa, et al., 2025; Katche, Makokha, Zachary, & Adaramola, 2023; Mufti, Irhamni, & Darnas, 2025; Selvakumar, Maawa, & Rusiyanto, 2025).

Despite these advances, many studies rely heavily on monthly average data or performance ratio (PR) metrics alone, which may not fully capture the operational dynamics of PV systems (Fitriyana, Rusiyanto, & Maawa, 2025; Gani, Zaki, Bahagia, Maghfirah, & Faisal, 2025; Kazem, Chaichan, Al-Waeli, & Sopian, 2024; Selvakumar, Gani, Xiaoxia, & Salleh, 2025). The lack of granular insights into daily or hourly behavior, power distribution, and thermal characteristics represents a gap in the literature particularly for small-scale residential or institutional systems in tropical environments (Efremov & Kumarasamy, 2025; Hosamo & Mazzetto, 2025; Khalisha, Caisarina, & Fakhrana, 2025; Muzakki & Putro, 2025). To address this limitation, several recent works have incorporated advanced performance visualization tools such as normalized loss diagrams, scatter plots, and frequency histograms (Irhamni, Kurnianingtyas, Muhtadin, Bahagia, & Yusop, 2025; Maghfirah, Yusop, & Zulkifli, 2025; Muhibbuddin, Hamidi, & Fitriyana, 2025; Rosdi, Maghfirah, Erdiwansyah, Syafrizal, & Muhibbuddin, 2025). However, the integration of these tools into a unified analytical framework remains limited. Furthermore, few studies explicitly examine how various energy levels and temperature-voltage behavior contribute to long-term output and system stability.

This study aims to fill that gap by offering a comprehensive, figure-based analysis of a 3000 Wp grid-connected PV system over a full one-year period. A total of 15 graphical visualizations are employed to assess energy input/output relationships, system losses, voltage and temperature distributions, and real-time power dynamics. This multi-dimensional approach provides both depth and clarity in evaluating PV performance beyond conventional monthly summaries. By combining traditional PR analysis with novel tail-distribution and histogram-based metrics, this research seeks to enhance understanding of PV behavior under real-world conditions. The study also emphasizes the importance of operational data collection in optimizing long-term performance and supporting system design in tropical regions.

The results contribute valuable benchmarks and performance patterns that can inform future system deployment strategies, energy forecasting models, and inverter selection guidelines. Importantly, the study was conducted without external funding, relying solely on author contributions—highlighting a grassroots approach to advancing solar research. The objective of this study is to assess the technical performance of a 3000 Wp photovoltaic system by analyzing actual operating data over one year. Key focus areas include energy yield, system losses, power distribution, thermal and electrical behavior, and overall efficiency trends. Through this, the study aims to offer a comprehensive performance reference for similar systems operating under tropical climatic conditions.

2. Methodology

System Description

The study was conducted on a grid-connected photovoltaic (PV) system with a nominal capacity of 3000 Wp, installed in a tropical region. The system comprises monocrystalline silicon modules configured to operate optimally under local irradiance and temperature conditions. The PV array is connected to a single-phase inverter, which converts the DC output into AC power for grid injection. The system is equipped with a data logging unit for real-time performance monitoring.

Data Collection

Performance data were collected continuously over a 12-month period, from January 1 to December 31. Parameters recorded include:

a. Global incident irradiance on the collector plane (W/m^2)
b. Reference incident energy ($kWh/m^2/day$)
c. Array voltage and power output (V and W)
d. System AC output (kWh/day)
e. Module temperature (°C)
f. System losses and performance ratio (PR)

Data were measured at high frequency and aggregated into daily and monthly values for further analysis. The data acquisition system ensured accuracy by using calibrated sensors and a certified inverter with built-in monitoring.

Performance Indicators

Key performance indicators (KPIs) used in the analysis include:

a. Reference yield (Yr): incident solar energy on module plane ($kWh/m^2/day$)
b. Final yield (Yf): usable energy output per kWp (kWh/kWp/day)
c. Performance ratio (PR): Yf/Yr
d. Collection loss (Lc) and System loss (Ls): derived from normalized performance data

Analytical Approach

The performance was evaluated using 15 graphical visualizations, including:

a. Monthly and daily energy input/output curves
b. Normalized loss diagrams
c. Frequency histograms of power, voltage, and temperature
d. Tail distribution graphs for irradiance and power
e. Correlation plots between irradiance and temperature

These figures were used to assess not only the energy yield but also the temporal and thermal behavior of the system, the power distribution profiles, and efficiency fluctuations over time.

Limitations and Assumptions

This study does not involve simulations or financial analysis. The focus is strictly on technical performance under real environmental conditions. The data and analysis are based solely on field measurements without external funding or third-party intervention.

3. Result & Discussion

Fig. 2 illustrates the monthly reference incident solar energy received on a photovoltaic (PV) array surface, expressed in kilowatt-hours per square meter per day ($kWh/m^2/day$). This parameter represents the average daily solar irradiance under standard reference conditions. The annual average value recorded is 4.846 $kWh/m^2/day$, which reflects a high level of solar energy availability and suggests that the location is favorable for solar PV system implementation. The graph reveals a clear seasonal trend. The highest solar irradiance occurs in February, reaching around 6.0 $kWh/m^2/day$, followed closely by January with approximately 5.8 $kWh/m^2/day$. These early-year months offer the greatest solar potential. In contrast, the lowest value appears in June, at approximately 4.0 $kWh/m^2/day$. This decline is likely due to increased cloud cover or reduced daylight hours during the monsoon or rainy season. After June, the solar energy gradually increases, peaking again in November at about 5.4 $kWh/m^2/day$.

These seasonal fluctuations have direct implications for PV system design and operation. During months with lower irradiance such as May through July solar energy production decreases, and thus energy storage systems or auxiliary power sources may be necessary to ensure a consistent energy supply. On the other hand, months with higher irradiance allow for optimal energy production, making them suitable for maximizing direct usage or charging storage systems. Overall, **Fig. 2** highlights the importance of considering seasonal solar resource variability when planning and optimizing PV systems. The relatively high annual average irradiance of 4.846 kWh/m²/day confirms the site's excellent potential for solar energy generation but also underscores the need for strategic system sizing and energy management throughout the year.

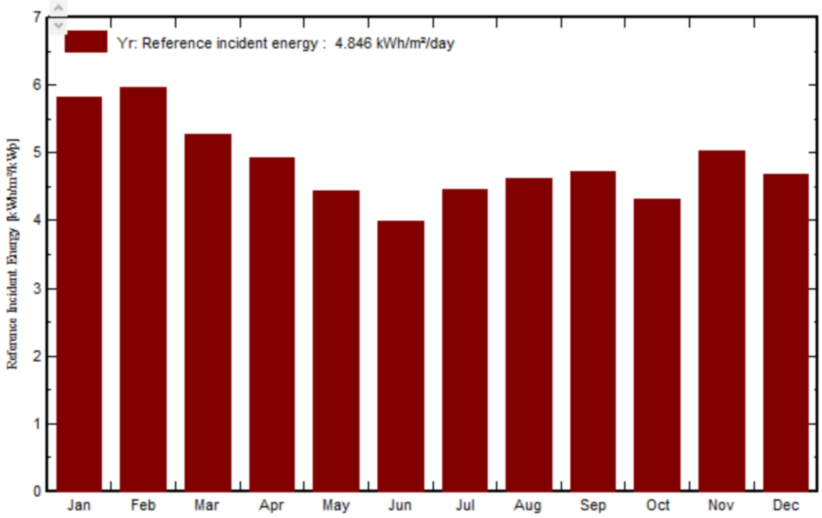

Fig. 2. Monthly Reference Incident Solar Energy Graph

Fig. 3 presents the monthly normalized photovoltaic (PV) energy production for a system with a nominal power of 3000 Wp, measured in kilowatt-hours per kilowatt-peak per day (kWh/kWp/day). The graph distinguishes between three key components of energy flow: the useful energy produced (Yf) shown in dark red, the system loss (Ls) due to inverters and other components shown in green, and the collection loss (Lc) resulting from PV array inefficiencies, shown in purple. On an annual basis, the values are summarized as follows: the produced useful energy is 4.06 kWh/kWp/day, system losses are 0.16 kWh/kWp/day, and collection losses amount to 0.63 kWh/kWp/day. The monthly trend aligns with seasonal solar availability, with the highest normalized production observed in February and January, and the lowest in June. These patterns reflect the same seasonal variation identified in the previous figure, where solar irradiance is highest at the beginning and end of the year and lowest during the middle months. Despite losses, the useful energy output remains relatively stable, indicating that the system performs consistently well under varying environmental conditions.

This figure is crucial for evaluating the performance efficiency of the PV system by showing how much of the incident solar energy is effectively converted into usable electrical output after accounting for technical losses. It highlights the importance of addressing both inverter efficiency and PV array performance to optimize system yield throughout the year. The relatively low total loss (0.79 kWh/kWp/day) suggests a well-functioning system with minimal energy waste.

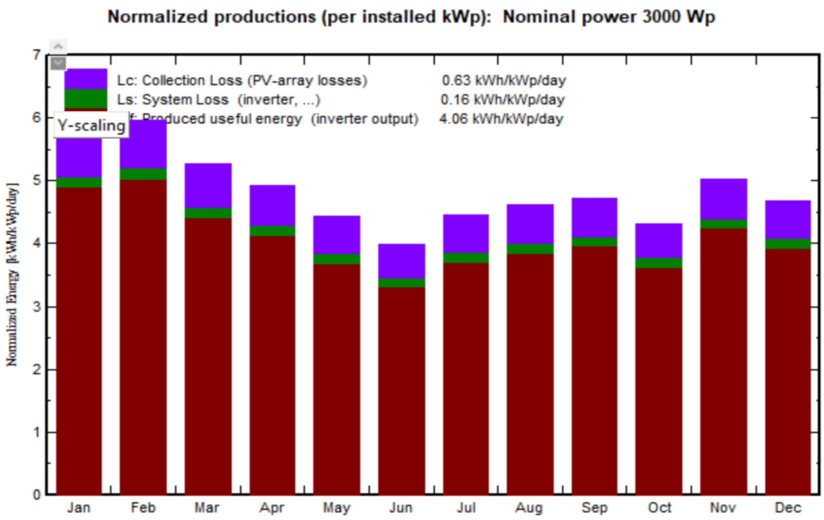

Fig. 3. Normalized PV Energy Production per Installed kWp (Nominal Power: 3000 Wp)

Fig. 4 displays the normalized production and loss factors for a photovoltaic (PV) system with a nominal capacity of 3000 Wp. The graph illustrates the monthly proportion of energy output (Yf) and system losses, normalized with respect to the total available energy. The dark red section represents the produced useful energy (Yf), while the green and purple portions indicate system loss (Ls) due to inverter inefficiencies and collection loss (Lc) due to PV array losses, respectively. The annual averages of these factors are as follows: 83.8% of the incoming solar energy is successfully converted into usable electrical energy (Yf), while 3.3% is lost in the inverter and other system components (Ls), and 12.9% is lost due to array-related issues such as thermal losses, dirt, mismatch, and irradiance angle losses (Lc). The graphical bars remain consistent across all months, indicating a stable and uniform performance of the PV system throughout the year regardless of seasonal variations.

This figure is significant because it emphasizes the efficiency and reliability of the PV system. The consistently high share of useful energy (above 83%) and relatively low losses (totalling 16.2%) reflect a well-designed and well-maintained system. Furthermore, the normalization approach allows performance evaluation independent of absolute irradiance values, making it easier to compare with other systems or locations.

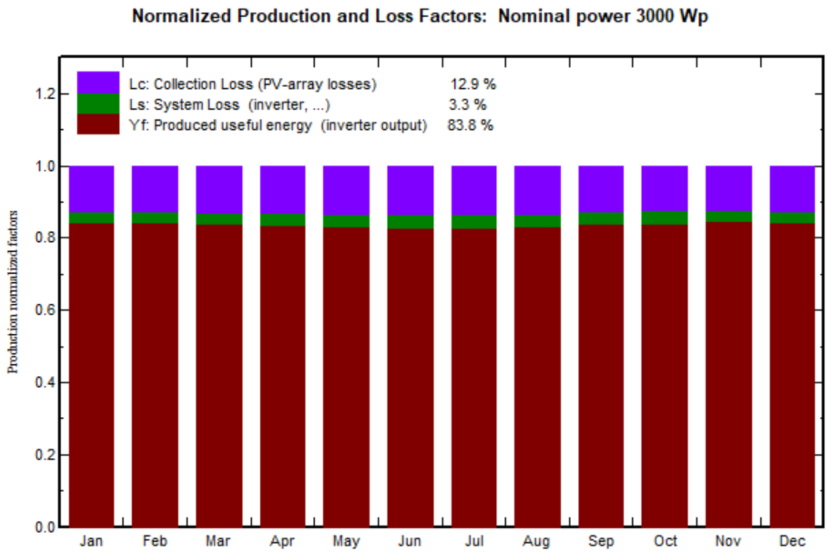

Fig. 4. Normalized Production and Loss Factors for PV System (Nominal Power: 3000 Wp)

Fig. 5 illustrates the Performance Ratio (PR) of a photovoltaic (PV) system with a nominal capacity of 3000 Wp. The PR is a dimensionless metric that measures the overall efficiency of a PV system by comparing the actual energy output (Yf) to the theoretical energy available from solar irradiance (Yr), according to the equation PR = Yf/Yr. A PR value close to 1.0 indicates an extremely efficient system, while lower values suggest energy losses within the system. In this chart, the annual average PR is 0.838, meaning that approximately 83.8% of the incident solar energy is successfully converted into usable electrical energy after accounting for system and environmental losses. Monthly PR values remain remarkably consistent throughout the year, ranging closely around the 0.83–0.84 mark. This stability demonstrates that the system performs reliably across different seasons, despite variations in solar irradiance and temperature.

The high and stable PR value confirms the good design, installation quality, and operational management of the PV system. It also reflects minimal impact from shading, temperature losses, or inverter inefficiencies. As a key performance indicator, PR is widely used in the solar industry to benchmark systems and assess long-term yield consistency. Therefore, this chart provides strong evidence of a well-functioning PV system with reliable performance over time.

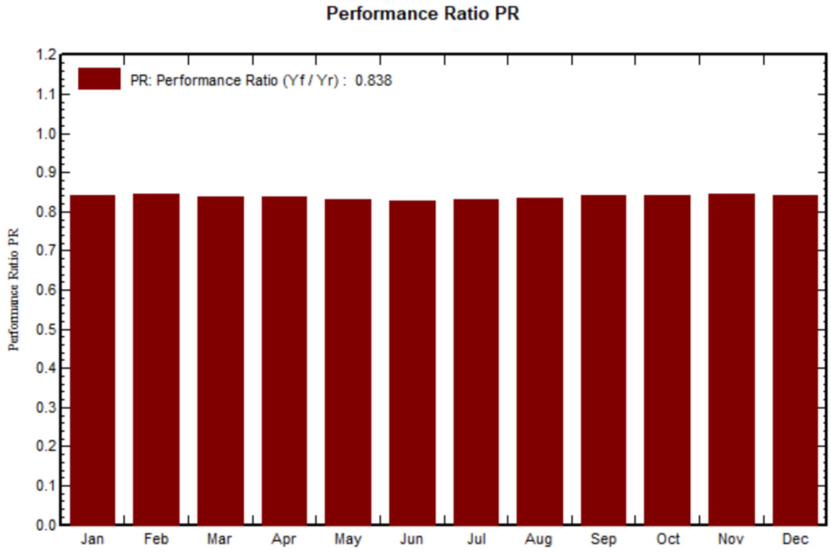

Fig. 5. Performance Ratio (PR) Chart for 3000 Wp PV System

Fig. 6 illustrates the distribution of incident solar irradiation on the collector plane over the course of one year, presented as a histogram. The x-axis represents the global irradiance on the collector plane in watts per square meter (W/m²), while the y-axis indicates the frequency of occurrence, given in kilowatt-hours per square meter per bin (kWh/m²/bin). This type of graph provides insight into how often specific irradiance levels are received by the PV system. From the distribution pattern, it is evident that irradiance values most frequently occur in the 600 to 900 W/m² range, where the histogram reaches its peak. This range represents the optimal operating condition for PV modules, where energy generation is high due to strong and consistent sunlight. On the other hand, very low irradiance levels (<200 W/m²) and extremely high values (>1000 W/m²) are relatively rare.

This distribution is valuable for assessing the expected performance and energy yield of a PV system. It helps system designers and operators understand how much time the array spends under different irradiance conditions and thus optimize component selection, system orientation, and energy management strategies. Overall, the figure confirms that the system location benefits from frequent high-irradiance conditions, which is advantageous for solar power generation.

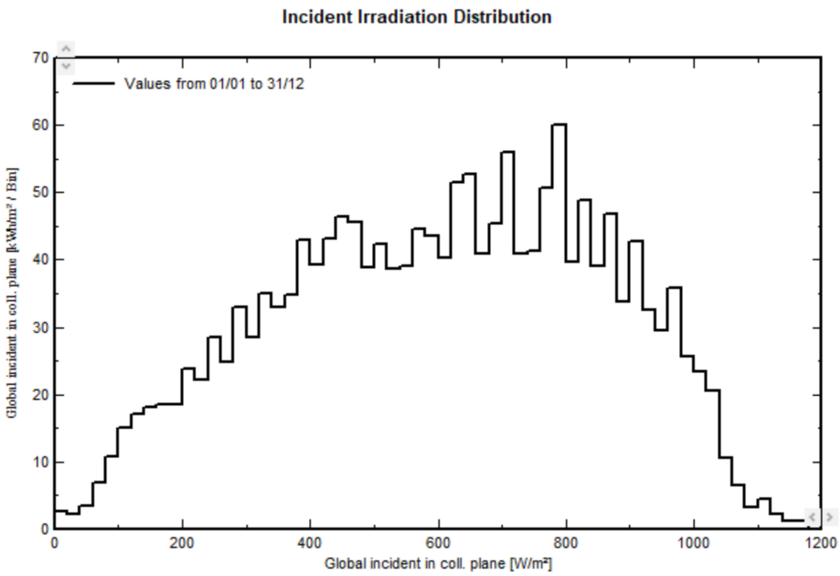

Fig. 6. Incident Irradiation Distribution on Collector Plane

Fig. 7 presents the incident irradiation tail distribution on the collector plane, providing a cumulative representation of global solar irradiance over a one-year period. The x-axis represents the irradiance intensity in watts per square meter (W/m²), while the y-axis shows the cumulative global incident energy in kilowatt-hours per square meter (kWh/m²). This tail distribution graph indicates the total amount of energy accumulated up to a specific irradiance threshold. The curve demonstrates a steep initial slope from 0 to about 600 W/m², where a large portion of the total annual solar energy is accumulated. Beyond this range, the curve gradually flattens, indicating that higher irradiance levels contribute less frequently to the total energy accumulation but still provide significant energy when they occur. For instance, irradiance above 800 W/m² contributes a smaller share of the total operational hours but delivers high power output when available.

This graph is particularly useful for system designers and analysts to evaluate how different irradiance levels contribute to the overall energy yield. It helps in understanding the operational efficiency range of the PV modules and supports decisions related to system sizing, performance prediction, and energy management strategies. The relatively smooth and consistent decline in the curve implies a balanced and predictable irradiance profile, favorable for efficient photovoltaic energy generation.

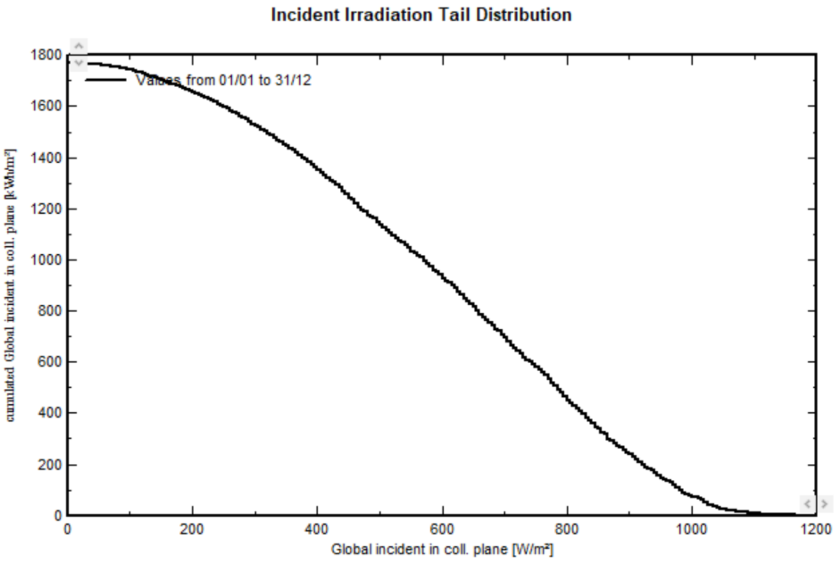

Fig. 7. Incident Irradiation Tail Distribution on Collector Plane

Fig. 8 shows the relationship between array temperature and effective irradiance throughout the year, visualized through a scatter plot. The x-axis represents the effective global irradiance corrected for incident angle modifier (IAM) and shading effects, in watts per square meter (W/m²), while the y-axis indicates the average module temperature during operation, in degrees Celsius (°C). Each black data point corresponds to a temperature-irradiance pair observed between January 1st and December 31st. The red dot represents the Standard Test Conditions (STC), where irradiance is 1000 W/m² and temperature is 25°C. The data distribution clearly demonstrates a positive linear correlation: as irradiance increases, the array temperature also rises. This is expected, as greater solar energy absorption leads to heating of the PV modules. Most of the observed temperatures range between 30°C and 60°C, with corresponding irradiance values mainly between 200 W/m² and 1000 W/m². The dense clustering of points indicates a consistent and predictable thermal response of the array to varying sunlight intensity.

Understanding this relationship is important because higher module temperatures reduce PV efficiency, as cell voltage drops with increasing temperature. This figure is crucial for assessing thermal performance, predicting energy output losses due to heat, and planning cooling or ventilation strategies to maintain system performance. The deviation of real operational conditions from the ideal STC point also emphasizes the importance of using field data for accurate performance modeling.

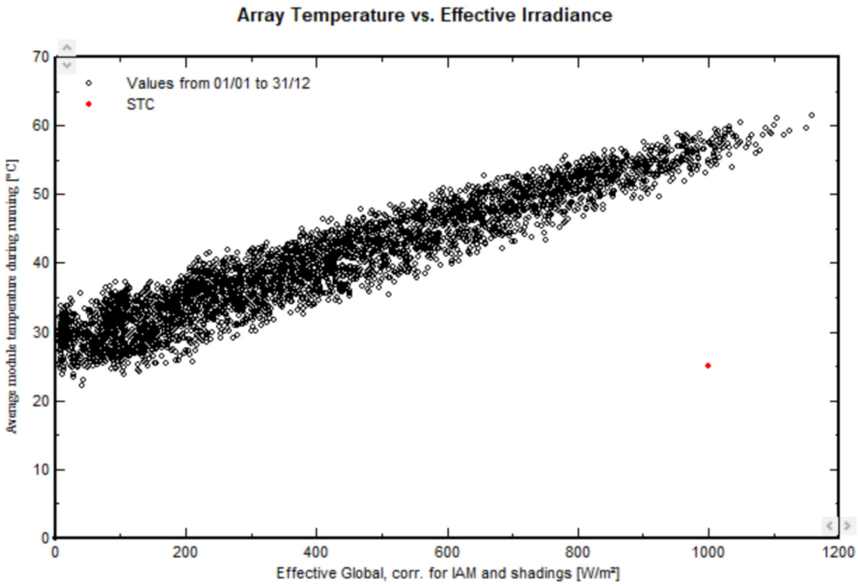

Fig. 8. Array Temperature vs. Effective Irradiance

Fig. 9 displays the daily solar energy input/output relationship for the PV system over the course of one year. The x-axis represents the daily global solar irradiation incident on the collector plane (in kWh/m²/day), while the y-axis shows the available solar energy output in kilowatt-hours per day (kWh/day). Each data point corresponds to a day's observation from January 1st to December 31st, capturing real-world operational behavior. The plot reveals a strong linear correlation between daily solar irradiance and system energy output. This linear trend indicates that the PV system responds consistently and proportionally to the amount of solar energy received. As irradiance increases, the amount of energy converted and made available by the system rises accordingly. The absence of significant scatter or deviation from the trendline implies minimal performance variability and efficient system operation across a range of irradiance levels.

This figure is critical for validating the predictability and responsiveness of the PV system. It suggests that the system behaves as expected under varying solar conditions, and energy output can be reliably estimated based on daily solar input. Such information is particularly valuable for energy forecasting, performance evaluation, and operational planning in both off-grid and grid-tied solar energy applications.

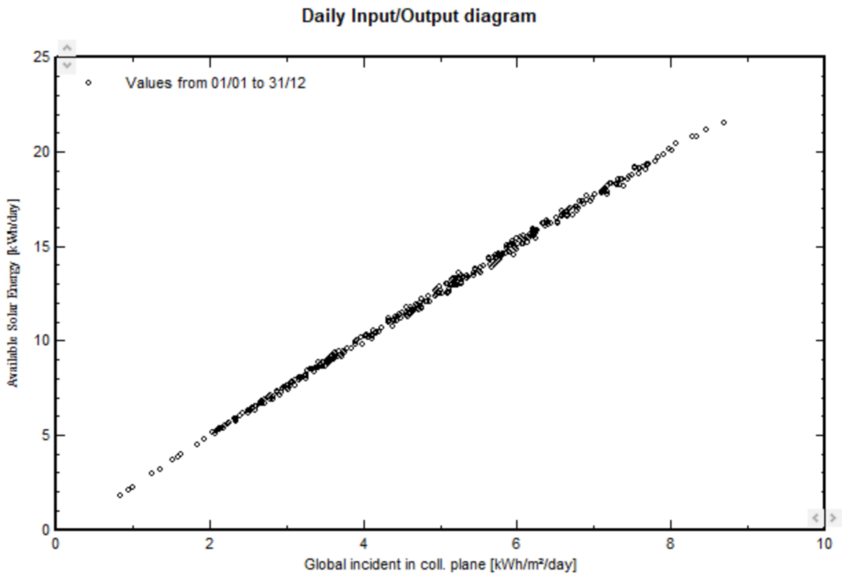

Fig. 9. Daily Solar Energy Input/Output Diagram

Fig. 10 presents the daily system output energy of the photovoltaic (PV) installation over the course of a full calendar year. The x-axis represents the time from January to December, while the y-axis indicates the available solar energy output per day in kilowatt-hours (kWh/day). Each vertical line reflects the system's daily energy production, which varies in response to solar conditions and weather patterns. The graph reveals significant day-to-day variability, with energy output ranging between approximately 2 kWh/day and over 20 kWh/day. This fluctuation is expected due to changing weather, cloud cover, and seasonal solar irradiance. The highest outputs are seen during January to March and October to December, corresponding to periods of higher solar irradiance and longer daylight hours. In contrast, the May to August period shows consistently lower and more fluctuating output, likely due to seasonal cloudiness or monsoonal effects, which reduce solar energy availability.

This figure provides a realistic view of operational energy yield, emphasizing the intermittent nature of solar power and the importance of storage or backup systems in maintaining consistent energy supply. Despite daily variability, the system demonstrates an overall reliable generation trend aligned with annual solar cycles, making it suitable for long-term planning and performance evaluation of solar PV systems.

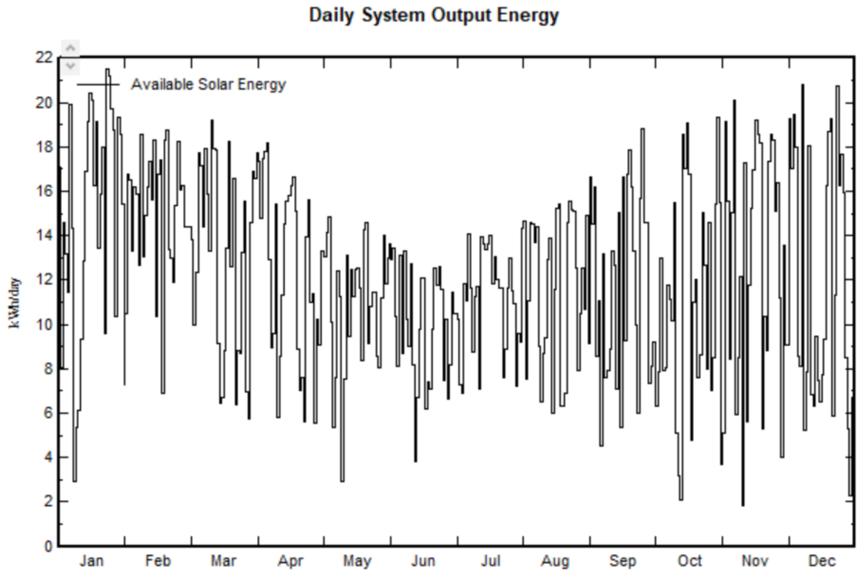

Fig. 10. Daily System Output Energy Graph

Fig. 11 illustrates the power distribution at the output of the photovoltaic (PV) array over the course of a year. The x-axis represents the effective power output of the array in watts (W), while the y-axis shows the frequency of occurrence in terms of energy contribution (kWh per bin). This histogram indicates how often the PV array operates at various power levels, providing insight into its typical working conditions. The graph shows that most of the array's power output occurs in the range between 1000 W and 2500 W, with a prominent peak around 2000 W. This peak suggests that the PV array frequently operates close to two-thirds of its nominal rated capacity (3000 Wp), reflecting a high level of performance and efficient utilization of solar input. Output below 500 W occurs less frequently, indicating that the system rarely experiences very low irradiance or shutdown conditions.

This distribution is valuable for evaluating the performance characteristics of the PV array, particularly its ability to maintain high output under variable irradiance conditions. A concentrated frequency around mid-to-high power levels signifies strong and consistent system performance. Moreover, it assists in estimating expected energy yield, designing inverter sizing, and optimizing load matching. Overall, the figure reflects a robust energy-generating profile typical of well-oriented and well-maintained solar arrays in a favorable irradiance environment.

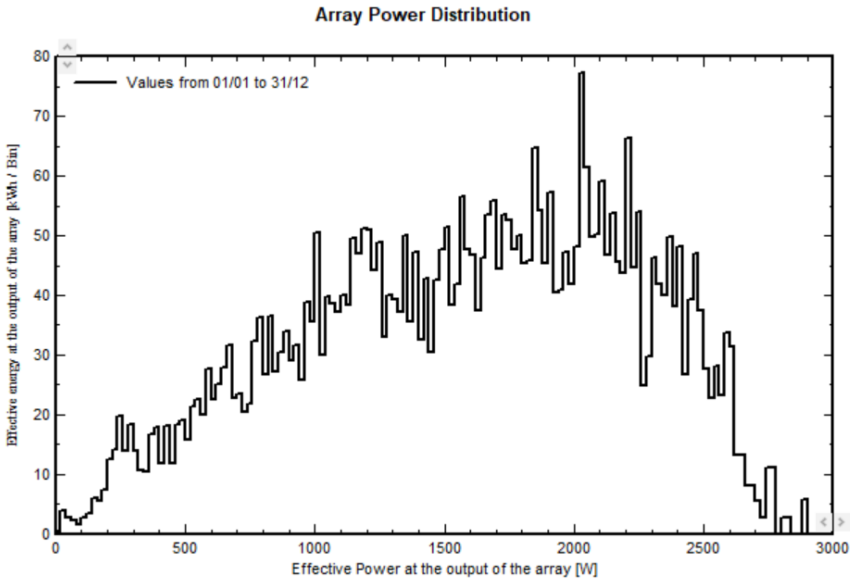

Fig. 11. Array Power Distribution

Fig. 12 shows the system output power distribution for the photovoltaic (PV) installation, covering the entire calendar year. The x-axis represents the available solar energy output in watts (W), while the y-axis shows the frequency of occurrence as energy contribution in kilowatt-hours per bin (kWh/bin). This histogram captures the behavior of the PV system after the energy passes through the inverter, i.e., the net AC power delivered to the load or grid. The power distribution curve exhibits a strong concentration of output between 1000 W and 2500 W, with a prominent peak around 2000 W, similar to the array-level distribution shown in the previous figure. However, some reduction in peak values is evident, which can be attributed to system-level losses, such as inverter efficiency and power conversion limitations. The system rarely produces output below 300 W, which implies minimal idle periods and confirms the reliability of solar resource availability.

This figure is important for evaluating the real-world energy yield of the system, providing insight into how often the system operates near its rated capacity and how inverter or other downstream components influence output. A well-shaped distribution with high energy contributions at mid-to-high power levels, as seen here, reflects a healthy and well-performing PV system. It also assists in optimizing energy dispatch strategies, inverter selection, and load matching to ensure efficient system integration and utilization.

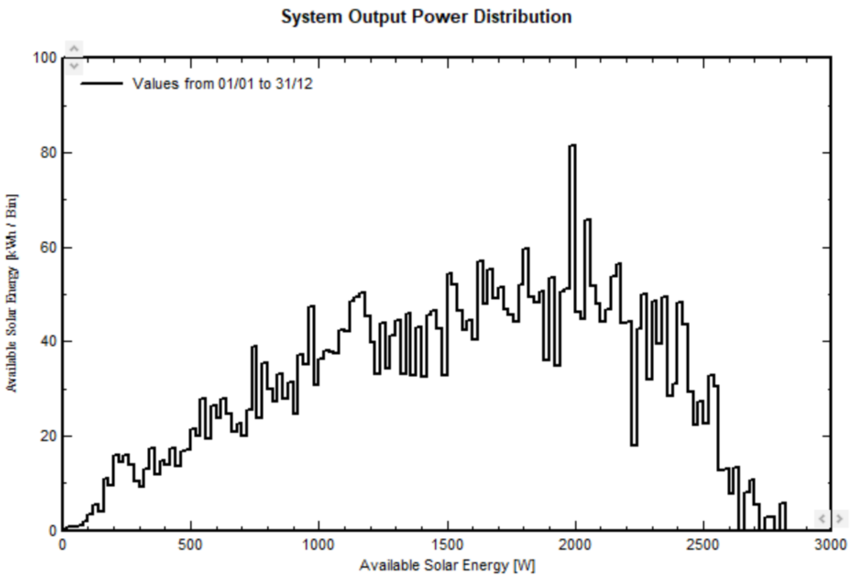

Fig. 12. System Output Power Distribution

Fig. 13 presents the tail distribution of system output power, showing the cumulative energy contribution of various power levels delivered by the PV system throughout the year. The x-axis represents the available system output power in watts (W), while the y-axis shows the cumulative solar energy output in watt-hours (Wh), integrated from January 1st to December 31st. The graph starts at the highest cumulative energy value and steadily declines as the available power increases, forming a smooth, downward-sloping curve. This indicates that a significant portion of the total energy is generated during lower to mid power levels, while higher power levels (above ~2000 W) contribute relatively less frequent but still valuable output. The tail becomes almost flat near 2800–3000 W, implying that operation near peak capacity is rare.

This figure is particularly useful for analyzing the performance dynamics and operating regime of the system. It helps quantify how much of the total annual energy is accumulated below or above specific power thresholds, which is vital for inverter sizing, energy dispatch modeling, and performance optimization. The gradual nature of the curve implies a well-distributed generation profile, affirming the system's ability to deliver energy efficiently across a range of solar conditions.

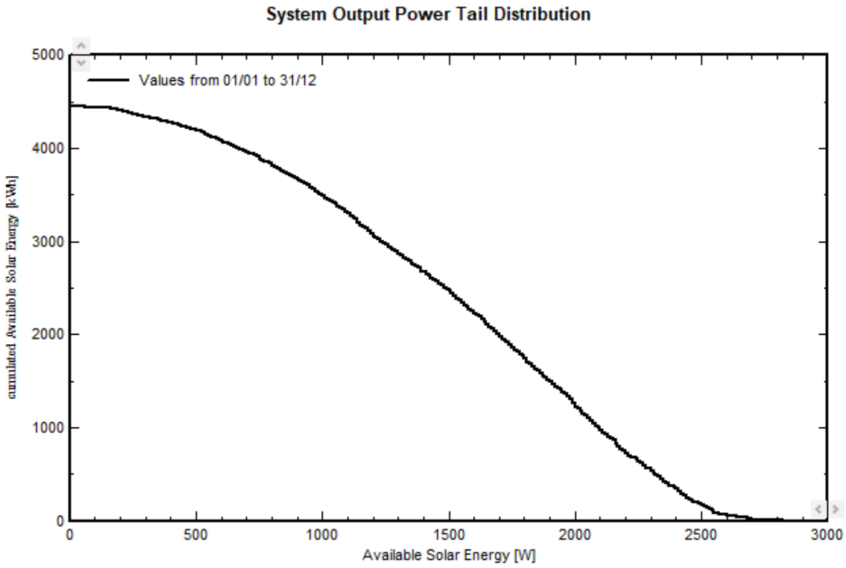

Fig. 13. System Output Power Tail Distribution

Fig. 14 illustrates the distribution of array voltage throughout the year, captured in the form of a histogram. The x-axis represents the array voltage in volts (V), while the y-axis shows the frequency of occurrence in hours per bin. This figure reflects the voltage behavior of the photovoltaic (PV) array during its operational period from January 1st to December 31st. The distribution reveals that most of the array voltage values are concentrated between 145 V and 155 V, with the highest frequency occurring around 150 V. This sharp peak indicates that the system consistently operates at or near an optimal voltage point for energy conversion, which is crucial for efficient maximum power point tracking (MPPT) by the inverter. Voltage values below 140 V or above 155 V are relatively rare, suggesting that the system rarely experiences extreme fluctuations.

This histogram is valuable for evaluating the stability and efficiency of the electrical characteristics of the PV array. A narrow and consistent voltage range, as shown in this graph, indicates good array configuration, low thermal or mismatch losses, and stable environmental operating conditions. This kind of distribution helps ensure that the inverter operates within its optimal input range, minimizing conversion losses and improving overall system performance.

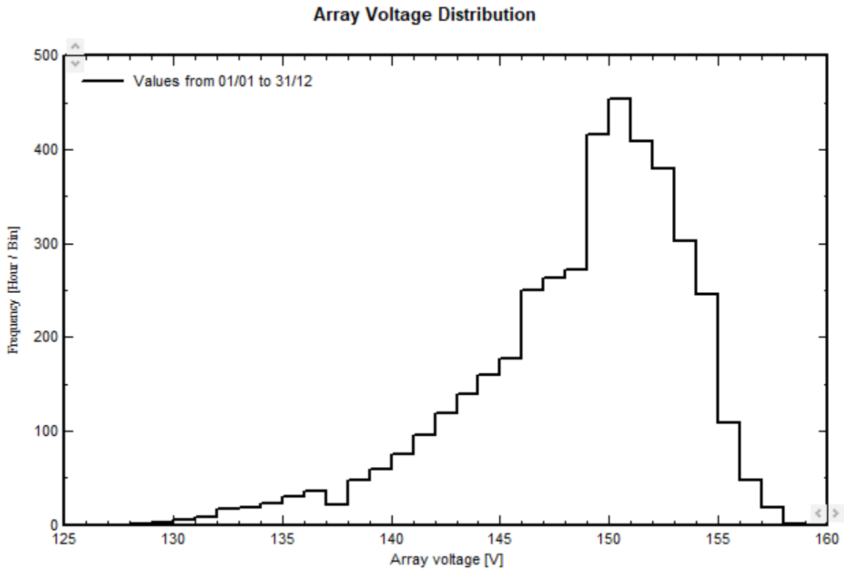

Fig. 14. Array Voltage Distribution

Fig. 15 presents the distribution of array temperatures recorded during PV system operation over a full year. The x-axis shows the average module temperature during running in degrees Celsius (°C), while the y-axis represents the frequency of occurrence in hours per bin. This histogram provides a clear view of how often the array operates within certain temperature ranges, offering valuable insight into the thermal behavior of the photovoltaic modules under actual environmental conditions. The distribution reveals that the most frequent temperature range lies between 30°C and 40°C, with the peak occurring around 35°C, indicating that the system often operates within a relatively moderate temperature zone. As the temperature increases beyond 40°C, the frequency gradually decreases, with some operations reaching up to 60°C. Temperatures below 25°C and above 60°C are extremely rare, confirming that extreme thermal conditions are infrequent at this installation site.

This data is crucial because module temperature significantly influences PV performance. Higher temperatures tend to reduce the voltage output of solar cells, thus decreasing overall system efficiency. Therefore, understanding the typical temperature distribution allows for better estimation of thermal losses, supports the planning of cooling strategies, and contributes to more accurate energy yield forecasting. The shape of the distribution in Figure 15 suggests a well-balanced thermal environment, supporting stable and predictable system performance.

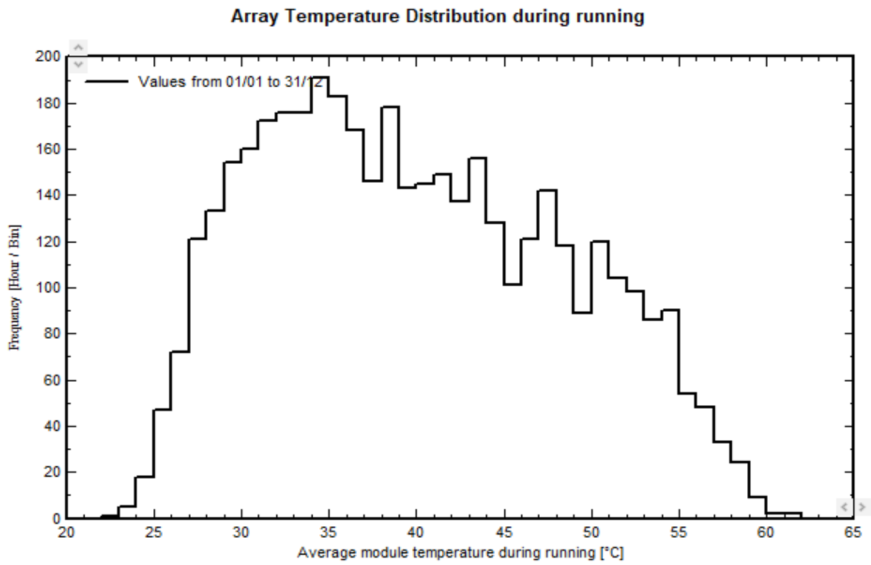

Fig. 15. Array Temperature Distribution During Running

This article offers a comprehensive and data-driven evaluation of a 3000 Wp photovoltaic (PV) system, highlighting several novel contributions to the field of solar energy performance analysis. The work stands out by integrating 15 distinct figures that collectively capture the full operational dynamics of the PV system from solar irradiance patterns to thermal behavior, electrical characteristics, and daily energy output. Unlike many previous studies that focus solely on monthly yield or PR values, this study delves deeper into the granular behavior of the system using hourly distributions, tail analyses, and scatter plots that reveal detailed interactions between irradiance, temperature, and power generation. For instance, the tail distribution graphs (**Figs. 7** and **13**) provide unique insights into how different levels of irradiance and output power cumulatively contribute to the system's annual energy yield an approach rarely visualized in such clarity.

Additionally, the correlation between array temperature and effective irradiance (**Fig. 8**) offers empirical validation of expected thermal responses, which is essential for modeling real-world degradation and efficiency. The article also contributes new perspective by presenting voltage and temperature frequency distributions (**Figs. 14** and **15**), which are often overlooked in PV performance reporting but are critical for inverter matching and thermal management strategies. Moreover, the normalized loss factor breakdown (**Figs, 3** and **4**) distinguishes the relative contributions of collection and system losses with a precision that can be used as a reference for system designers and energy planners seeking to optimize layout or component selection. The stable performance ratio (**Fig. 5**) further reinforces the reliability of the system across seasonal variations, strengthening the case for adopting similar system configurations in comparable climatic zones.

In conclusion, the novelty of this article lies in its integrated performance visualization approach, the depth of statistical insight derived from real operational data, and the practical implications drawn for system design, sizing, and optimization. The findings not only enhance the understanding of system behavior under varying environmental and load conditions but also establish a reproducible framework for future PV performance assessment studies.

4. Conclusion

This study comprehensively analyzed the performance of a 3000 Wp photovoltaic (PV) system using real operational data recorded throughout a full calendar year. The findings provide clear insights into the system's energy yield, efficiency, thermal characteristics, and operational behavior under varying environmental conditions. The system achieved an annual average reference incident energy of 4.846 kWh/m²/day, with the highest values observed in February (6.0 kWh/m²/day) and the lowest in June (4.0 kWh/m²/day), reflecting seasonal solar irradiance patterns. The produced useful energy averaged 4.06 kWh/kWp/day, while total system losses amounted to 0.79 kWh/kWp/day, consisting of 12.9% collection loss and 3.3% system (inverter) loss. This resulted in a high and consistent Performance Ratio (PR) of 0.838, indicating that 83.8% of the available solar energy was effectively converted into usable electrical output. The power distribution analysis showed that the system most frequently operated at power outputs between 1500 W and 2500 W, peaking around 2000 W at both the array and system output levels. Tail distribution plots confirmed that a significant share of annual energy was contributed by mid-range power levels, with infrequent operation near nominal capacity (3000 Wp), which is typical under real-world irradiance conditions. Thermal performance analysis indicated that the array temperature ranged primarily between 30°C and 50°C, peaking at around 35°C, with a clear positive correlation between irradiance and module temperature. The voltage distribution showed that the system predominantly operated at 145–155 V, with the most frequent voltage near 150 V, ensuring inverter compatibility and consistent DC performance. Daily input/output and output energy graphs demonstrated strong linearity and temporal alignment with seasonal irradiance, while also highlighting variability caused by daily weather patterns. The stable output throughout the year, despite fluctuating solar conditions, confirms the system's robustness and reliability. In summary, the system performed efficiently across all seasons, maintaining high conversion efficiency, thermal stability, and voltage consistency. The integration of detailed statistical analyses such as frequency, tail, and correlation plots offers a more nuanced understanding of PV system behavior. These findings serve as a valuable reference for improving future PV designs, performance modeling, and long-term energy forecasting.

Acknowledgement

The authors would like to express their sincere gratitude for the collaborative efforts that made this research possible. This study was conducted without any external funding support. All activities, including data collection, system monitoring, analysis, and manuscript preparation, were fully supported and contributed by the authors themselves as a collective academic contribution to the field of renewable energy.

References

Aghaei, M., Fairbrother, A., Gok, A., Ahmad, S., Kazim, S., Lobato, K., … Kettle, J. (2022). Review of degradation and failure phenomena in photovoltaic modules. *Renewable and Sustainable Energy Reviews*, 159, 112160. Retrieved from https://doi.org/https://doi.org/10.1016/j.rser.2022.112160

Bahagia, B., Nizar, M., Yasin, M. H. M., Rosdi, S. M., & Faisal, M. (2025). Advancements in Communication and Information Technologies for Smart Energy Systems and Renewable Energy Transition: A Review. *International Journal of Engineering and Technology (IJET)*, 1(1), 1–29.

Bhavani, M., Vijaybhaskar Reddy, K., Mahesh, K., & Saravanan, S. (2023). Impact of variation of solar irradiance and temperature on the inverter output for grid connected photo voltaic (PV) system at different climate conditions. *Materials Today: Proceedings*, 80, 2101–2108. Retrieved from https://doi.org/https://doi.org/10.1016/j.matpr.2021.06.120

Efremov, C., & Kumarasamy, S. (2025). Optimisation of Microgrid by HOMER Pro Software Design: Innovative Approach and Performance Evaluation. *International Journal of Engineering and Technology (IJET)*, 1(1), 120–130.

Fitriyana, D. F., Rusiyanto, R., & Maawa, W. (2025). Renewable Energy Application Research Using VOSviewer software: Bibliometric Analysis. *International Journal of Science & Advanced Technology (IJSAT)*, 1(1), 92–107.

Gani, A., Saisa, S., Muhtadin, M., Bahagia, B., Erdiwansyah, E., & Lisafitri, Y. (2025). Optimisation of home grid-connected photovoltaic systems: performance analysis and energy implications. *International Journal of Engineering and Technology (IJET)*, 1(1), 63–74.

Gani, A., Zaki, M., Bahagia, B., Maghfirah, G., & Faisal, M. (2025). Characterization of Porosity and Pore Volume in EFB Samples through Physical and Morphological Parameters. *International Journal of Engineering and Technology (IJET)*, 1(1), 90–99.

Hosamo, H., & Mazzetto, S. (2025). Data-Driven Ventilation and Energy Optimization in Smart Office Buildings: Insights from a High-Resolution Occupancy and Indoor Climate Dataset. *Sustainability*, 17(1), 58.

Iqbal, I., Rosdi, S. M., Muhtadin, M., Erdiwansyah, E., & Faisal, M. (2025). Optimisation of combustion parameters in turbocharged engines using computational fluid dynamics modelling. *International Journal of Simulation, Optimization & Modelling*, 1(1), 63–69.

Irhamni, I., Kurnianingtyas, E., Muhtadin, M., Bahagia, B., & Yusop, A. F. (2025). Bibliometric Analysis of Renewable Energy Research Trends Using VOSviewer: Network Mapping and Topic Evolution. *International Journal of Engineering and Technology (IJET)*, 1(1), 75–82.

Jalaludin, H. A., Kamarulzaman, M. K., Sudrajad, A., Rosdi, S. M., & Erdiwansyah, E. (2025). Engine Performance Analysis Based on Speed and Throttle Through Simulation. *International Journal of Simulation, Optimization & Modelling*, 1(1), 86–93.

Katche, M. L., Makokha, A. B., Zachary, S. O., & Adaramola, M. S. (2023). A comprehensive review of maximum power point tracking (mppt) techniques used in solar pv systems. *Energies*, 16(5), 2206.

Kazem, H. A., Chaichan, M. T., Al-Waeli, A. H. A., & Sopian, K. (2024). Recent advancements in solar photovoltaic tracking systems: An in-depth review of technologies, performance metrics, and future trends. *Solar Energy*, 282, 112946. Retrieved from https://doi.org/https://doi.org/10.1016/j.solener.2024.112946

Khalisha, N., Caisarina, I., & Fakhrana, S. Z. (2025). Mobility Patterns of Rural Communities in Traveling Traveling from The Origin Area to the Destination. *International Journal of Science & Advanced Technology (IJSAT)*, 1(1), 108–119.

Maghfirah, G., Yusop, A. F., & Zulkifli, Z. (2025). Using VOSviewer for Renewable Energy Literature Analysis: Mapping Technology and Policy-Related Research. *International Journal of Engineering and Technology (IJET)*, 1(1), 83–89.

Mufti, A. A., Irhamni, I., & Darnas, Y. (2025). Exploration of predictive models in optimising renewable energy integration in grid systems. *International Journal of Science & Advanced Technology (IJSAT)*, 1(1), 47–61.

Muhibbuddin, M., Hamidi, M. A., & Fitriyana, D. F. (2025). Bibliometric Analysis of Renewable Energy Technologies Using VOSviewer: Mapping Innovations and Applications. *International Journal of Science & Advanced Technology (IJSAT)*, 1(1), 81–91.

Muhtadin, M., Rosdi, S. M., Faisal, M., Erdiwansyah, E., & Mahyudin, M. (2025). Analysis of NOx, HC, and CO Emission Prediction in Internal Combustion Engines by Statistical Regression and ANOVA Methods. *International Journal of Simulation, Optimization & Modelling*, 1(1), 94–102.

Muzakki, M. I., & Putro, R. K. H. (2025). Greenhouse Gas Emission Inventory at Benowo Landfill Using IPCC Method. *International Journal of Science & Advanced Technology (IJSAT)*, 1(1), 18–28.

Pranoto, H., Rusiyanto, R., & Fitriyana, D. F. (2025). Sustainable Wastewater Management in Sumedang: Design, Treatment Technologies, and Resource Recovery. *International Journal of Science & Advanced Technology (IJSAT)*, 1(1), 38–46.

Rosdi, S. M., Maghfirah, G., Erdiwansyah, E., Syafrizal, S., & Muhibbuddin, M. (2025). Bibliometric Study of Renewable Energy Technology Development: Application of VOSviewer in Identifying Global Trends. *International Journal of Science & Advanced Technology (IJSAT)*, 1(1), 71–80.

Selvakumar, P., Gani, A., Xiaoxia, J., & Salleh, M. R. (2025). Porosity and Pore Volume Analysis of EFB Fiber: Physical Characterization and Effect of Thermal Treatment. *International Journal of Engineering and Technology (IJET)*, 1(1), 100–108.

Selvakumar, P., Maawa, W., & Rusiyanto, R. (2025). Hybrid Grid System as a Solution for Renewable Energy Integration: A Case Study. *International Journal of Science & Advanced Technology (IJSAT)*, 1(1), 62–70.

Yana, S., Mufti, A. A., Hasiany, S., Viena, V., & Mahyudin, M. (2025). Overview of biomass-based waste to renewable energy technology, socioeconomic, and environmental impact. *International Journal of Engineering and Technology (IJET)*, 1(1), 30–62.